Study of structural relaxation of metallic glasses by stress-free dilatometry

1989 J. Phys.: Condens. Matter 1 8305

(http://iopscience.iop.org/0953-8984/1/44/003)

J. Phys.: Condens. Matter 1 (1989) 8305–8318. Printed in the UK

Study of structural relaxation of metallic glasses by stress-free dilatometry

H Friedrichs† and H Neuhäuser
Institut für Metallphysik und Nukleare Festkörperphysik, Technische Universität, D-3300 Braunschweig, Federal Republic of Germany

Received 21 October 1988, in final form 6 April 1989

Abstract. Thermal expansion and structural relaxation during annealing of various metallic glass ribbons has been measured in a specially designed dilatometer avoiding any transfer rods and any tensile stress on the specimen. The spectra of activation energies for atomic rearrangements during structural relaxation up to crystallisation are determined for $Fe_{40}Ni_{40}B_{20}$, $Co_{66}Fe_4(MoSiB)_{30}$ and $Ni_{78}Si_8B_{14}$ alloys. The relaxation behaviour of specimens cut from different positions in a 50 mm wide ribbon of $Ni_{72}Si_8B_{20}$ indicates different cooling characteristics in the centre and near the edges of the ribbon, and a pronounced anisotropy along and perpendicular to the ribbon axis.

1. Introduction

The structure of amorphous alloys (metallic glasses) obtained by rapid quenching from the melt is in metastable equilibrium and is known to lower its energy by structural relaxation even at moderate heating in the amorphous state (e.g. Chen 1983, Egami 1983). This structural relaxation consists of a slight rearrangement of the atomic positions, connected with some densification (e.g. Chen 1978, Gerling and Wagner 1983, Pratten 1981) and is accompanied by a change in many of the physical properties.

More sensitive than direct density measurements is dilatometry (e.g. Girt *et al* 1980, Girt 1982, Leonardsson 1983, Sinning *et al* 1985, Mulder *et al* 1984, Huizer and van den Beukel 1987) which, however, if performed in conventional set-ups, may be disturbed by creep of the specimen at high temperatures on account of the external tensile stress applied to straighten the thin ribbon (Girt *et al* 1982, Leonardsson 1985). We have recently developed a simple arrangement which avoids this problem and in addition provides detection of length change directly in the furnace avoiding uncontrolled expansion of transfer rods (Neuhäuser *et al* 1985). If the structural relaxation occurs isotropically, from the measured change in length $\Delta l/l$, the change in density $\Delta\rho/\rho = 3\Delta l/l$ can be determined. In the following we report on some applications of this system to study the spectra of activation energy for structural relaxation (cf Gibbs *et al* 1983, Bothe and Neuhäuser 1982, 1983, Dietz and Börngen 1983, Bothe 1985a, b) of various types of metallic glasses, and in addition show an anisotropy of structural relaxation of melt-spin ribbons.

† Present address: Dräger-Werk AG, Moislinger Allee 53–55, D-2400 Lübeck, Federal Republic of Germany.

0953-8984/89/448305 + 14 $02.50

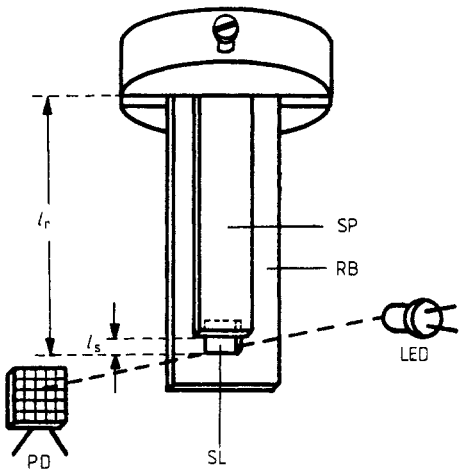

Figure 1. Principle of the experimental set-up for stress-free dilatometry (SP, specimen; RB, reference blade with slit SL; LED, light emitting diode modulated by a carrier frequency of 5 kHz; PD, photodiode).

2. Experimental procedure

The principle of stress-free dilatometry is indicated in figure 1. The change in length of the specimen is transformed into an optical signal by comparing its thermal expansion with that of a well known material (e.g., Cu, Ni, Mo). The free end of the specimen covers part of the rectangular hole ($1.0 \times 0.5\ \text{mm}^2$) in the reference blade. Due to the different expansion of specimen and reference, the width of the slit SL changes and this is monitored with high sensitivity by measuring the total transmitted light intensity (Neuhäuser *et al* 1985). Accounting also for the lateral expansion of the slit, the length change of the specimen can be calculated from the change of the output voltage $U(T)$ according to

$$\frac{\Delta l}{l(T_0)} = \frac{l(T) - l(T_0)}{l(T_0)} = \frac{l_r(T_0)(1 + \alpha(T)T - \alpha(T_0)T_0)}{l_r(T_0) - l_s(T_0)} - \frac{\{U(T)l_s(T_0)/[U(T_0)(1 + \alpha(T)T - \alpha(T_0)T_0)]\}}{l_r(T_0) - l_s(T_0)} - 1 \tag{1}$$

where T_0 is the temperature at the start of the experiment (usually room temperature), l_r and α denote the length and the thermal expansion coefficient, respectively, of the reference blade (see figure 1) and l_s is the width of the slit.

The main problem with this simple and inexpensive device consists in achieving a uniform illumination intensity across the few tenths of a mm which the whole system moves during thermal expansion of its components. This was realised by a defocusing lens and several scattering glasses between LED and slit. The sensitivity of intensity measurement by phase-sensitive amplification of the modulated (5 kHz) light signal is high enough to permit a short time resolution of length changes down to 2×10^{-7} m (using a slit width of $l_s \approx 0.2$ mm) and a long time resolution of about 2×10^{-6} m. With a reference length $l_r = 25$ mm relative length changes of $\Delta l/l = 5 \times 10^{-5}$ can be measured at an accuracy of 1%. An important limiting factor is the uncertainty in the value of α for the reference material (cf Nix and McNair 1941). Good temperature stabilisation of the LED and photodiode is required.

The device shown in figure 1 is surrounded by a furnace (cf Neuhäuser *et al* 1985)

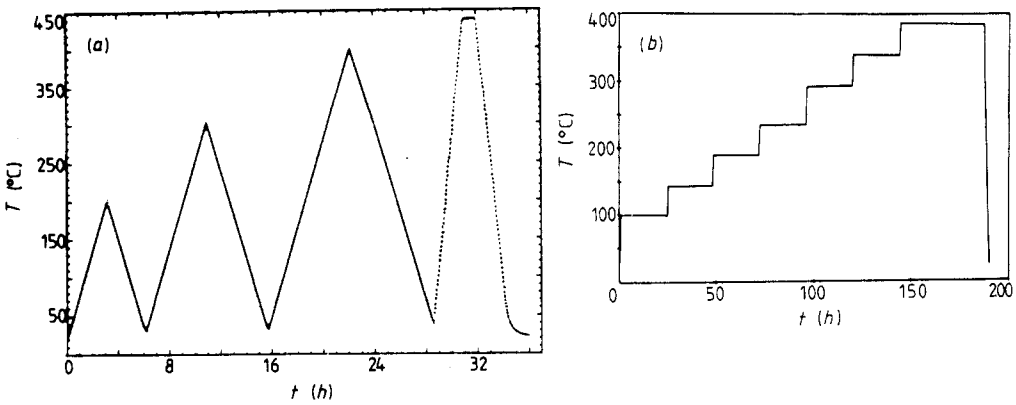

Figure 2. Two types of typical temperature programmes performed in the experiments: (*a*) constant heating rate; (*b*) stepwise isothermal heating.

inside a vacuum vessel with windows. This allows temperatures between room temperature and 450 °C to be reached at maximum rates of $dT/dt = \pm 10\ K\ min^{-1}$. Temperature programming and control (accuracy ±0.5 K) is realised by a simple personal computer. Two different types of experiments were performed: (i) measurements with constant heating rates (figure 2(*a*)), typically $\pm 1\ K\ min^{-1}$, and (ii) measurements with isothermal step heating (figure 2(*b*)).

In (i) several heating cycles with increasing maximum temperatures were usually applied in order to obtain reference curves for the various amorphous states achieved after partial structural relaxation. Figure 3(*a*) gives an example. After nearly linear expansion up to about 100 °C, similar to any material, the metallic glass exhibits less expansion because shrinking by structural relaxation sets in and is superimposed on the thermal expansion. The latter can be measured exclusively during cooling or during the second heating run up to a temperature slightly below the former maximum. The reversibility (at not too high a heating/cooling rate) indicates that the structural relaxation has occurred completely in this temperature interval. At higher temperature further structural relaxation takes place. After shifting the curves to a common origin at room temperature, their difference gives the total effect of structural relaxation. At sufficiently high temperature crystallisation sets in with a shrinking effect noticeably exceeding that during structural relaxation.

Figure 3(*b*) shows an example of the second type of measurements. The isothermal periods for 24 h are preselected to increasing temperatures reached by rapid heating ($5\ K\ min^{-1}$) from the previous step. These steps show up in figure 3(*b*) as the short vertical parts of the curve, indicating the decrease in length during isothermal heating. This decrease is displayed in figure 3(*c*) as a function of log(time) for one example at $T = 251$ °C to show the tendency towards a logarithmic time law characteristic of a wide distribution of activation energies (Gibbs *et al* 1983, Bothe and Neuhäuser 1983). The procedure (ii) takes, of course, a much longer time to fully cover the whole spectrum of activation events, but it provides a rather direct evaluation of this spectrum from the observed relaxation kinetics, as will be shown in § 3.

The measurements were performed with various types of metallic glasses obtained from Vacuumschmelze Hanau.

(i) VITROVAC 0040 ($Fe_{40}Ni_{40}B_{20}$), a magnetic material which shows severe annealing embrittlement. Thickness 35–40 μm, width 10.5 mm. Shiny side amorphous, on dull

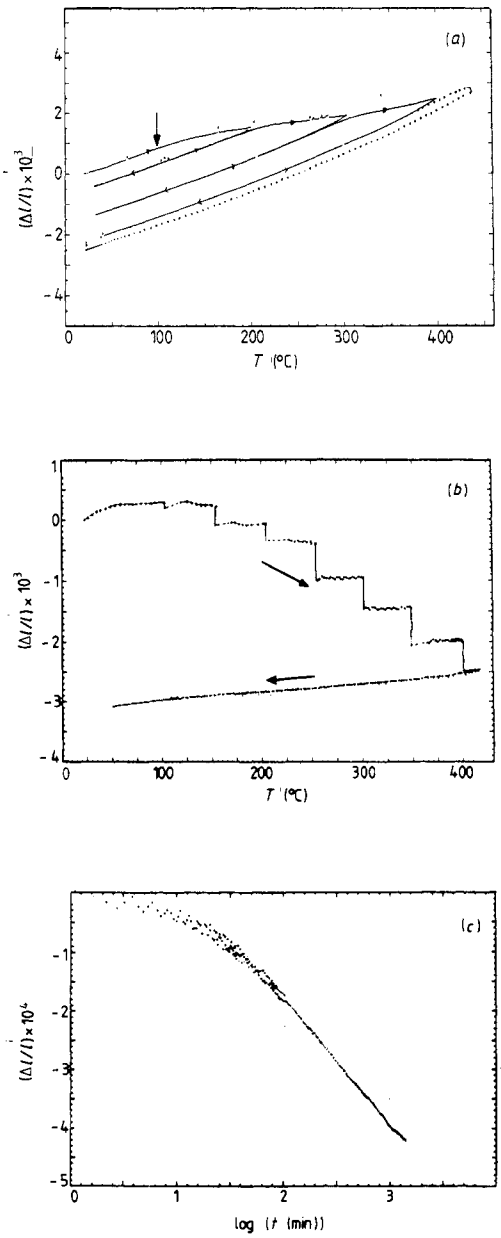

Figure 3. (*a*) Thermal expansion and superposed structural relaxation measured in an experiment with constant heating (and cooling) rate ($\dot{T} = 1$ K min^{-1}) (cf figure 2(*a*)) for the metallic glass VITROVAC 6025 ($Co_{66}Fe_4(MoSiB)_{30}$). The vertical arrow indicates the onset of structural relaxation. (*b*) Temperature dependence of the relative length change in an experiment with stepwise isothermal heating (cf figure 2(*b*)) for VITROVAC 6025. (*c*) Relative length change during one of the isothermal periods ($T = 251$ °C) of experiment (*b*) plotted against log (time).

side indication of some surface crystallites in x-ray diffraction. These surface crystallites (cf Hang Nam Ok and Morrish 1981a, b, Gonser *et al* 1983, Janot *et al* 1983), which can be removed by slight etching or polishing, grow only slowly during structural relaxation while the main body of the specimen remains amorphous.

(ii) VITROVAC 6025 ($Co_{66}Fe_4(MoSiB)_{30}$), a magnetic material designed with a minimum coefficient of magnetostriction (Hilzinger *et al* 1979). Thickness 40 μm, width 2.5 mm. Shiny side indicating some surface crystallisation, dull side amorphous according to x-ray diffraction. Contrary to (i), in this case heterogeneous nucleation at the

wheel during solidification appears to be less important than the slower quenching rate at the free surface of the ribbon. Apart from this difference, during annealing similar behaviour as for (i) was observed.

(iii) VITROVAC 0080 ($Ni_{78}Si_8B_{14}$), a paramagnetic material without severe annealing embrittlement. Thickness 30–35 μm, width 10.3 mm. Dull side mostly amorphous, shiny side indicating some surface crystallisation (cf Zuercher and Morris 1988a, b) with similar characteristics as for (i).

(iv) 50 mm wide ribbon of $Ni_{72}Si_8B_{20}$, thickness 55 μm, both sides amorphous according to x-ray diffraction.

3. Activation energy spectra of irreversible structural relaxation

As indicated above (figure 3(*c*)), the results of structural relaxation suggest that an extended distribution of relaxation times (or corresponding activation energies) exists for the processes of atomic rearrangements in the amorphous state. One aim of the present investigation is to characterise these spectra which are required for predictions of the changes in property with temperature and time. The method for extracting the spectra from measured kinetics traces back to Primak (1955) and is sketched briefly in the following.

3.1. Formalism

The elementary processes of structural relaxations are assumed to follow the rate equation

$$-\partial q/\partial t = K(T)\,(q(t) - q_\infty(t))^n \tag{2}$$

where q denotes the number (or density) of elements waiting at time t for the relaxation process to occur; q_∞ is the number (or density) approached at infinite time; n is the order of the reaction and $K(T)$ the kinetic function. We assume $n = 1$ and a *linear* connection between the observable *change* in a property p with change in number (or density) of relaxing units (cf Primak 1955, Gibbs *et al* 1983, Bothe and Neuhäuser 1983); thus

$$-\mathrm{d}p(E, t)/\mathrm{d}t = \nu \exp(-E/kT)p(E, t) \tag{3}$$

assuming an Arrhenius expression for each activation energy E of the distribution of relaxing units. In (3) we assume an energy- and temperature-independent attempt frequency ν, and neglect a possible change in q_∞ with temperature, which is a reasonable approximation for irreversible relaxation, but has to be considered for reversible relaxation processes (Gibbs *et al* 1983, Hygate and Gibbs 1987). According to Primak (1955), for isothermal experiments the differential equation (3) is solved by

$$p(E, t) = p_0(E) \exp(-\nu t \exp(-E/kT)) \tag{4}$$

with initial value p_0, and the *measured* change in the property is by integration over all contributing energies:

$$P(t)|_T = \int_0^{E_{\max}} (p_0(E) - p(E, t))\,\mathrm{d}E = \int_0^{E_{\max}} p_0(E)\theta_a(E, T, t)\,\mathrm{d}E \tag{5}$$

where $E_{\max}$ denotes the upper limit of the spectrum of activation energies and $\theta_a(E, T, t)$

is the so called annealing function $\theta_a = 1 - \exp(-\nu t \exp(-E/kT))$, which approaches a jump function, rising rapidly from 0 to 1 around $E = E_0 = kT \ln \nu t$.

The case of experiments with constant heating rate $\dot{T}$ (figure 2(*a*)) has also been evaluated by Primak (1960), who found approximately

$$P(T)|_{\dot{T}} = \int_0^{E_{max}} p_0(E)(1 - \exp\{-\nu(T/\dot{T})[1/(2 + E/kT)] \exp(-E/kT)\})\, dE$$

$$= \int_0^{E_{max}} p_0(E)\theta_t(E, T, \dot{T})\, dE. \tag{6}$$

From measurements of either $P(t)|_T$, i.e. the property change with time at various fixed temperatures, or $P(T)|_{\dot{T}}$, i.e. the property change with temperature (or time) at constant heating rate, the initial distribution of activation energies of the relaxing units, $p_0(E)$, can be determined by inversion of the integral equations (5) or (6), respectively. A very first impression can be obtained by approximating θ_a (or θ_t) by a step function rising at $E_0 = kT \ln \nu t$ (or about $kT \ln \nu(T/\dot{T})$). Then time t and temperature T define the characteristic energy E_0 up to which (nearly) all units have already relaxed, i.e. with increasing time and temperature the spectrum of activation energies is scanned through from its lowest to higher values.

3.2. Evaluation

The initial distribution of activation energies $p_0(E)$ is determined by numerical solution of the integral equations (5) and (6), which are discretised according to the discrete measured values of $P(T, t)$. In the procedure devised by Bothe (1985a, b) the vector $\boldsymbol{p}_0(E)$ is evaluated from the vector of measured values $\boldsymbol{P}$ and the matrix of the annealing function $\boldsymbol{\theta}_a$ or $\boldsymbol{\theta}_t$ using the least-squares method:

$$|\boldsymbol{P} - \boldsymbol{\theta}_{a,t}\boldsymbol{p}_0|^2 = \text{minimum}. \tag{7}$$

Oscillations of the solution are suppressed according to Phillips (1962) by requiring for the second derivative of $\boldsymbol{p}_0$ for E:

$$\int (p_0''(E))^2\, dE = \text{minimum}. \tag{8}$$

This requirement is added to (7) with a Lagrangian parameter λ (Bothe 1985a, b). The appropriate value of λ is estimated by performing the whole calculation using a known test spectrum and looking for the best fit. It turns out that λ may be changed by about one order of magnitude without any significant effect on the fitted spectrum. Satisfactory results for the fitting procedure were obtained for constant heating rate measurements by using $\lambda = 1$ or 0.1, by discretising the energy scale into 40 steps and using 250–450 measured values.

An important point in the evaluation is the determination of the attempt frequency ν which is *a priori* unknown. Therefore the calculation is performed assuming different values of ν and looking for the minimum standard deviation of the fit.

4. Results and discussion

Spectra of activation energies for structural relaxation using the change of elastic modulus (measured by the vibrating-reed technique) have been evaluated earlier (Bothe

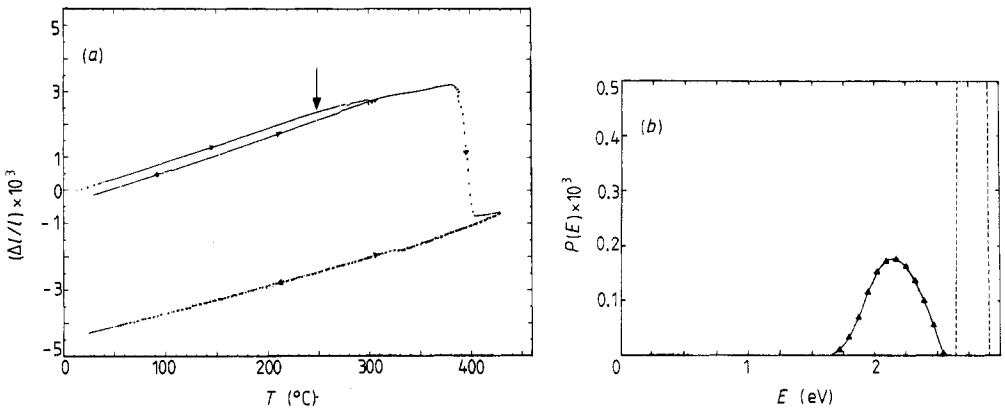

Figure 4. (*a*) Thermal expansion of VITROVAC 0040 ($Fe_{40}Ni_{40}B_{20}$) in an experiment according to figure 2(*a*) ($\dot{T} = 1$ K min^{-1}) showing structural relaxation for $T \geqslant 270$ °C and crystallisation at 380 °C. The vertical arrow indicates the onset of structural relaxation. (*b*) Spectrum of activation energies for structural relaxation and for crystallisation (between broken lines) evaluated from figure 4(*a*). Attempt frequency $\nu = 3.2 \times 10^{14}$ s^{-1}.

1985a, b) applying the stepwise isothermal heating method (figure 2(*b*)). The change in length by structural relaxation is usually less than 4% of the change in frequency (or modulus) (Bothe *et al* 1985, Dietz *et al* 1984) and therefore more difficult to measure and evaluate. In the following, we will determine spectra from the length change during experiments at constant heating rate (figure 2*a*) of various metallic glasses.

4.1. $Fe_{40}Ni_{40}B_{20}$

In figure 4 the measured curves (*a*) and the evaluated spectrum (*b*) are shown for VITROVAC 0040 ribbons. At a heating rate of $\dot{T} = 1$ K min^{-1} the change in length by structural relaxation can be resolved only for temperatures exceeding 270 °C. This is in accord with the observations of Gordelik and Sommer (1985), who found a minimum change in length for the alloy of this composition, 0040. The high temperature for structural relaxation infers a relatively high activation energy of 1.6 eV at the onset of the spectrum $p_0(E)$ (cf figure 4(*b*)); $p_0(E)$ extends up to about 2.5 eV. The uncertainties in these energy values can be estimated to about ± 0.2 eV. In an experiment with considerably lower heating rate, $\dot{T} = 0.2$ K min^{-1}, the onset of structural relaxation was observed at a slightly lower temperature, as expected; the calculated spectrum agrees well with that in figure 4(*b*).

In the calculation of these energies the value of the attempt frequency ν enters critically. The minimum standard deviation of the fit results in $\nu = 3.2 \times 10^{14}$ s^{-1} with an uncertainty of a factor of about 3. This value is of the order of atomic vibration frequencies and thus would suggest mono-atomic jumps in the relaxation processes. A quite similar spectrum and a similar attempt frequency was determined by Sommer *et al* (1985) from DSC measurements. Huizer and van den Beukel (1987) concluded from recent dilatometric measurements on $Fe_{40}Ni_{40}B_{20}$ that about 90% of the observed shrinking effect is of irreversible nature (only part of this could be explained by the free volume theory with a fixed activation energy of 2.6 eV) and extends over an energy range of 1.4 to 2.5 eV, in reasonable agreement with figure 4(*b*).

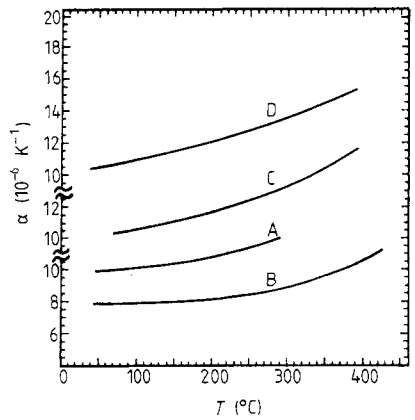

Figure 5. Temperature dependence of the thermal expansion coefficient $\alpha\,(=\mathrm{d}(\Delta l/l)/\mathrm{d}T)$ for relaxed amorphous (A) and for crystallised (B) VITROVAC 0040 ($Fe_{40}Ni_{40}B_{20}$), for relaxed amorphous VITROVAC 6025 ($Co_{66}Fe_4(MoSiB)_{30}$) (C), and for relaxed amorphous and for crystallised VITROVAC 0080 ($Ni_{78}Si_8B_{14}$) (D).

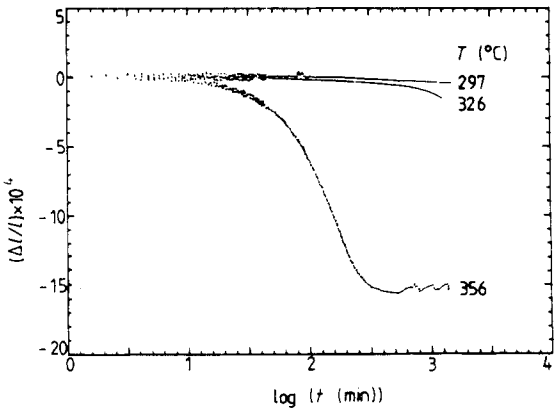

Figure 6. Kinetics of structural relaxation and crystallisation of VITROVAC 0040 ($Fe_{40}Ni_{40}B_{20}$) during several isothermal steps in an experiment according to figure 2(*b*).

The thermal expansion coefficients α of the relaxed ($\alpha = 9.9 \times 10^{-6}\,\mathrm{K}^{-1}$ at $T = 300$ K) and of the crystallised ($\alpha = 7.8 \times 10^{-6}\,\mathrm{K}^{-1}$ at $T = 300$ K) material differ by about 20% (figure 5); this tendency is expected from the difference in density and is in accord with observations in the literature (e.g., Gordelik and Sommer 1985, Steinberg *et al* 1980a, b). The absolute α values agree only roughly with those from the literature (Cahn *et al* 1984, Grössinger *et al* 1984, Gordelik 1983, Mulder *et al* 1984, Huizer and van den Beukel 1987); the differences might be due to magnetostrictive effects caused by different magnetic domain structures and magnetic fields during heating, and/or due to slight differences in alloy composition.

Crystallisation occurs around 380 °C (at $\dot{T} = 1\,\mathrm{K\,min}^{-1}$) and is connected with a large densification of the material (figure 4(*a*)) (cf Gerling and Wagner 1983, Gordelik and Sommer 1985); the corresponding peak in the spectrum is centred around 2.6–2.9 eV in agreement with reported data (Sommer *et al* 1985, Scott 1978, Stubicar *et al* 1977). In the isothermal step heating programme (figure 2(*b*)) the crystallisation of the same material occurs during the step at $T = 356$ °C and seems already to be initiated during the step at 326 °C (in figure 6, showing the isothermal kinetics in the ln t plot. This is consistent with x-ray diffraction observations which, after a 24 h anneal at 350 °C, indicated distinct further growth of surface crystallites on the dull side of the specimen and initiation of crystallites on the shiny side (cf § 2(i)). The x-ray diagrams of both sides still differ after 72 h of annealing at 400 °C because of the complicated transformation

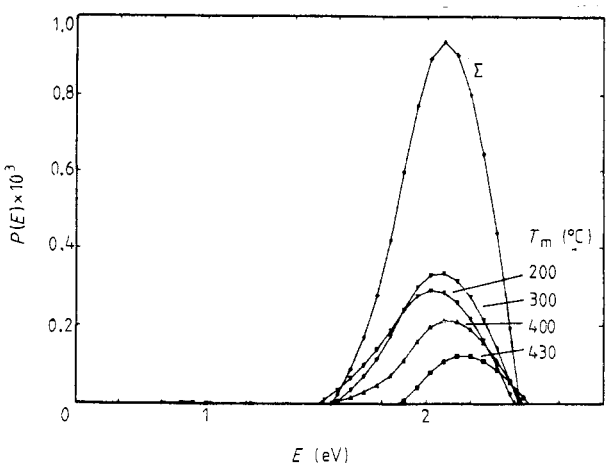

Figure 7. Spectra of activation energies for structural relaxation of VITROVAC 6025 ($Co_{66}Fe_4(MoSiB)_{30}$) evaluated for each heating cycle in Fig. 3a), and sum spectrum of these partial spectra. The attempt frequencies yielding best fit for each cycle are, respectively, $\nu(T_{max} = 200\,°C) = 10^{15}\,s^{-1}$, $\nu(T_{max} = 300\,°C) = 10^{14}\,s^{-1}$, $\nu(400\,°C) = 10^{11.5}\,s^{-1}$, $\nu\,(430\,°C) = 10^{11.5}\,s^{-1}$.

of crystalline phases (cf Stubicar *et al* 1977, Steffen and Liedtke 1981, Müller and von Heimendahl 1982).

4.2. $Co_{66}Fe_4(MoSiB)_{30}$

The spectrum of activation energies for structural relaxation in VITROVAC 6025 is determined from the measurement shown in figure 3(*a*) using successive runs with constant heating rates up to increasing maximum temperatures. Each of the four runs is evaluated separately and yields the partial spectra shown in figure 7 and the following attempt frequencies ν: $\nu(T_{max} = 200\,°C) = 10^{15}\,s^{-1}$, $\nu\,(300\,°C) = 10^{14}\,s^{-1}$, $\nu\,(400\,°C) = 10^{11.5}\,s^{-1}$, $\nu\,(430\,°C) = 10^{11.5}\,s^{-1}$. According to the much earlier onset of structural relaxation effects in figure 3(*a*) (6025) as compared with figure 4(*a*) (0040), the lowest energy values in the spectrum for 6025 (figure 7) are around 1.2 eV (cf figure 4(*b*)), while it extends up to similar energy values of about 2.5 eV. With increasing maximum annealing temperatures in the successive heating/cooling runs, the onset of further relaxation shifts to higher energies as expected; the total spectrum can be taken as the sum of the partial spectra in figure 7; it agrees well with that determined from a single run performed up to 430 °C which yields for the best fit an attempt frequency of $\nu = 10^{13}\,s^{-1}$. This corresponds well with the average value of the attempt frequencies evaluated above from step experiments. This analysis demonstrates that the assumption of a constant frequency ν in the calculation according to § 3 is still rather crude and has to be improved. Due to the increasing number of parameters, however, it will hardly be possible to introduce spectra for the activation energy as well as for the attempt frequency (cf Nowick and Berry 1972). The decrease of ν with increasing temperature indicates that atomic clusters of increasing size are involved in the thermally activated rearrangement processes.

Crystallisation of VITROVAC 6025 was not achieved with the available furnace; therefore we cannot compare the thermal expansion coefficient, which is $\alpha = 10.5 \times 10^{-6}\,K^{-1}$ at room temperature and increases slightly with T up to 250 °C in the amorphous state (cf figure 5), with that of the crystallised sample. The thermal expansion coefficient α increases very strongly for $T \geq 250\,°C$, which corresponds to the Curie temperature. This indicates the influence of magnetic effects in this material which is optimised for very low magnetostriction (Hilzinger *et al* 1979).

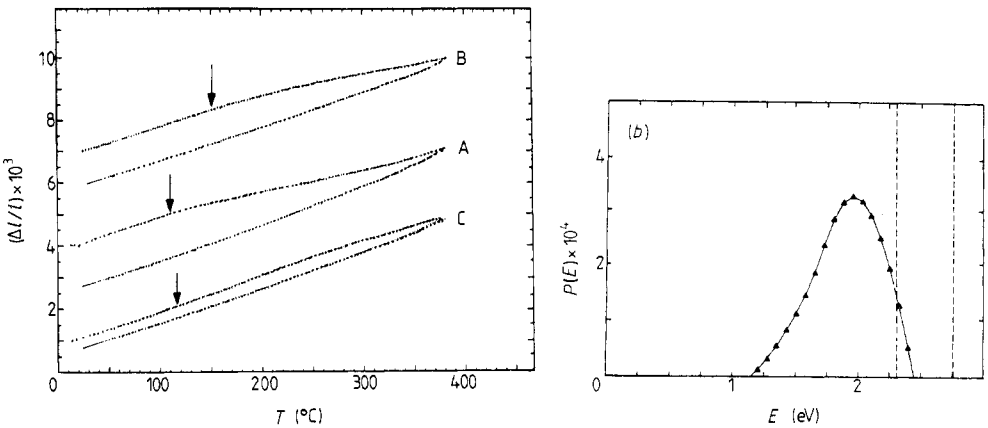

Figure 8. (*a*) Measured length change during several heating/cooling cycles for VITROVAC 0080 ($Ni_{78}Si_8B_{14}$) ($\dot{T} = 1$ K min^{-1}). The vertical arrow indicates the onset of structural relaxation. (*b*) Spectrum of activation energies for structural relaxation and crystallisation (between broken lines) evaluated from (*a*). Attempt frequency $\nu = 10^{11}$ s^{-1}.

4.3. $Ni_{78}Si_8B_{14}$

Comparison of the behaviour of this amorphous alloy VITROVAC 0080 with the previous ones is of interest because it contains only one type of metallic atoms and therefore is not expected to show a contribution from chemical short-range order (CSRO) to structural relaxation (Komatsu *et al* 1983). Figures 8(*a*) and 8(*b*) show the measured length change and the evaluated spectrum of activation energies, respectively, for structural relaxation and crystallisation (the part of the peak within broken lines). As with all the other spectra shown previously, and also those determined from other properties (Bothe 1985a, b), the part due to structural relaxation is clearly separated from the crystallisation peak by a 'valley' in the frequency distribution of energies. Structural relaxation in this material sets in only for $T > 200$ °C (at a heating rate of $\dot{T} = 1$ K min^{-1}), corresponding to an activation energy of 1.1 eV, and extends again up to about 2.5 eV. The attempt frequency (which depends on T much less than that for VITROVAC 6025 (§ 4.2)) is determined by the fit to $\nu = 10^{11}$ s^{-1} which indicates that large groups of atoms are involved in the relaxation processes (cf Bothe and Neuhäuser 1983). This low value of ν implies, according to the characteristic energy $E_0 = kT \ln \nu t = kT \ln \nu T/\dot{T}$, a higher temperature for the onset of structural relaxation in figure 8(*a*) (NiSiB) as compared with figure 3(*a*) (Co-FeMoSiB).

The coefficient of thermal expansion α increases slightly with temperature from $\alpha = 10.5 \times 10^{-6}$ K^{-1} (300 K), and does not show a difference between the relaxed amorphous and the crystallised condition, contrary to $Fe_{40}Ni_{40}B_{20}$ (figure 5). This may be due to the absence of magnetic effects and to the absence of a change in CSRO in $Ni_{78}Si_8B_{14}$ with no significant change in the atomic potentials (cf the $\Delta\alpha$ effect which has been observed in Invar alloys and explained by a change in the number of Fe–Fe pairs (Fukamichi 1983)).

Crystallisation occurs at $T = 430$ °C (at $\dot{T} = 1$ K min^{-1}) with an activation energy around 2.5 eV in agreement with the literature (Morris 1983, 1984, Pilz and Ryder 1985, Komatsu *et al* 1983) and produces a change in length exceeding that of structural relaxation by a factor of five, but is smaller than that in § 4.1 for $Fe_{40}Ni_{40}B_{20}$. As indicated above, the structural relaxation in $Ni_{78}Si_8B_{14}$ is believed to consist mainly in a change of topological short-range order which is measured in $\Delta l/l$ directly as the loss of free

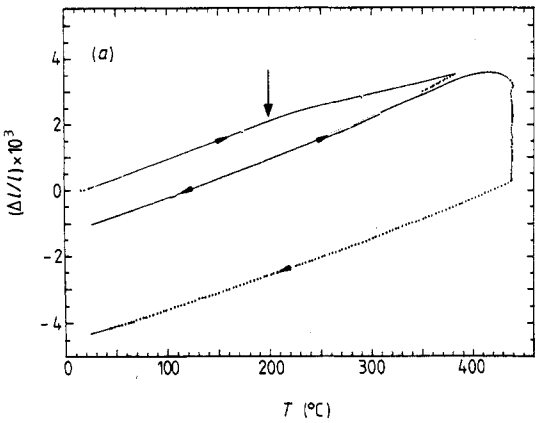

Figure 9. Changes in length measured during heating and cooling ($\dot{T} = 1$ K min^{-1}) for three different specimens cut from a 50 mm wide ribbon of $Ni_{72}Si_8B_{10}$. Specimen cut along the axis of the ribbon in its centre (A) and at its edges (B), and cut perpendicular to the axis (C). The curves are shifted along the ordinate for clarity. Vertical arrows indicate the onset of structural relaxation.

volume. The crystallisation of this alloy has been studied by various authors, e.g., Pilz and Ryder (1985), Reusswig *et al* (1984) and Baro *et al* (1988). Recent careful investigations by Zuercher and Morris (1988) on the surface and bulk crystallisation of a glass of similar composition ($Ni_{76}Si_7B_{17}$), produced under clean and fast cooling conditions, reveal the importance of the surface composition which may differ markedly from the bulk promoting surface crystallisation (Koester and Herold 1981). In the first stage of crystallisation nucleation at grown-in embryos (probably short-range ordered arrangements of the alloying elements) may occur, and this may interfere with the later stages of structural relaxation.

4.4. $Ni_{72}Si_8B_{20}$

This material was available as a ribbon of width 50 mm and therefore offered the possibility to check easily the isotropy of structural relaxation. In spite of its large thickness of 55 μm, the material is amorphous on both sides. Several specimens of 6×33 mm^2 were cut (A) in the centre along the ribbon axis, (B) at the edge along the axis, and (C) perpendicular to the ribbon axis. The corresponding traces of length change during heating and cooling at constant rate ($\dot{T} = 1$ K min^{-1}) are shown in figure 9.

The relaxation processes set in at a much lower temperature (110 °C) for specimen A cut along the centre axis than for specimen B (150 °C) cut along the edges. This can be explained by the experience (Hilzinger 1986) that for such wide ribbons their outer parts leave the melt-spinning wheel earlier than the centre part. The latter is therefore cooled down more rapidly, while the outer parts already feel an annealing treatment during production due to slower cooling in the air.

The total relaxation effect of specimen C cut perpendicular to the axis in the centre of the ribbon is much smaller than that along the axis (A). From around 110 °C, when the shrinking along the axis sets in, a very slight expansion normal to the ribbon axis is observed, which for $T \geqslant 250$ °C is overcome by the overall shrinking effect. The cooling curves of all specimens A, B and C coincide, indicating that the anisotropy disappears during annealing.

Quite similar observations have been reported for $Fe_{40}Ni_{40}B_{20}$ by Sinning *et al* (1985) and for $Ni_{78}Si_8B_{14}$ by Leonardsson (cited by Sinning *et al* (1985)). These findings suggest that an anisotropy of the density exists in the as-quenched material as a consequence of

the highly directional production process, which seems to leave more loosely packed regions of elongated shape in the matrix of average density. An anisotropy is also expected in the direction of ribbon thickness (cf Kopmann *et al* 1983). If the volume fractions of these ellipsoidal or elongated disc-shaped regions differ in the direction of their long and short axes, the observed effect (figure 9) could be explained. Neutron small-angle scattering experiments by Yavari *et al* (1982, 1984, 1985) and by Steeb and Lamparter (1985) in fact indicate the existence of elongated regions with different density than the average value. They may be produced from fluctuations in density of the melt when it hits the rapidly moving surface of the melt-spinning wheel, where these regions are sheared and frozen in rapidly (Yavari and Desre 1984).

The observation of this anisotropy of course prevents a direct connection between the measured length change and the average change of density. On the other hand, the density measurements cannot be related directly to simple structural relaxation processes, in particular since they may occur in each direction with different activation energies and amounts.

5. Conclusions

A new dilatometric technique has been developed and applied to measure the release of free volume during structural relaxation and crystallisation of various metallic glasses. The method avoids any tensile stress on the ribbon and thus measures thermal expansion without any contribution from creep. As the change in length is measured directly in the furnace by an optical principle, it is free from the disturbing effects of expanding transfer elements applied in usual dilatometers. The materials compared include the magnetic amorphous alloys VITROVAC 0040 ($Fe_{40}Ni_{40}B_{20}$) and VITROVAC 6025 ($Co_{66}Fe_4(MoSiB)_{30}$), the latter being optimised for near-zero magnetostriction, and the paramagnetic VITROVAC 0080 ($Ni_{78}Si_8B_{14}$) containing only one type of metallic atoms implying negligible CSRO. The temperature programmes of the annealing procedure were selected to either heating at constant rate of temperature increase (and decrease) or stepwise heating with 24 h isothermal periods. According to a formalism introduced by Primak (1955, 1960) these measurements can be evaluated to yield the spectra of activation energies for structural relaxation, i.e. local rearrangements of atoms or atom groups.

The character of these spectra is the same for all glassy metals investigated (cf also Bothe 1985a, b): after a sharp onset at 1.1–1.6 eV (depending on alloy composition and pre-annealing history) the part of the spectrum corresponding to structural relaxation extends continuously (roughly parabola shaped) up to about 2.5 eV. Slightly above this energy a sharp peak in the spectrum occurs which corresponds to crystallisation. Both parts of the spectrum are slightly overlapping, but they are separated by a valley in the frequency distribution of energies.

Details of the atomic processes occurring during structural relaxation are not yet clear. They involve topological as well as chemical short-range ordering (cf Egami 1983, Huizer and van den Beukel 1987) with release of free volume which has been measured directly here. It is also possible that a small contribution to the observed effect at high temperatures is due to surface crystallisation which is known to occur well before crystallisation of the bulk (Koester and Herold 1981) and appears to be connected with some change of the chemical composition in the surface region (Janot *et al* 1983, Zuercher and Morris 1988). The shrinkage by crystallisation in the surface region exerts

a compressive stress in the bulk material (Gonser *et al* 1983, Hang Nam Ok and Morrish 1981a, b). This could cause some plastic relaxation during annealing at high temperature; it can be estimated to be negligible in our case of relatively short annealing programmes at constant heating rate.

The attempt frequency in the Arrhenius ansatz used to describe the relaxation kinetics is determined from the fits of the spectrum to the measurements. Its value indicates the character of the atomic rearrangements: in $Fe_{40}Ni_{40}B_{20}$ they seem to involve atomic jumps ($\nu \approx 10^{14}$ s^{-1}), while in $Ni_{78}Si_8B_{14}$ ($\nu \approx 10^{11}$ s^{-1}) groups of atoms are supposed to be involved in each activated process. Measurements of partial spectra in $Co_{66}Fe_4(MoSiB)_{30}$ indicate that in the amorphous state ν decreases with increasing temperature. This point has to be clarified in further investigations.

The amorphous alloy $Ni_{72}Si_8B_{20}$ was available as a 50 mm wide ribbon enabling a check on the isotropy of structural relaxation. Specimens cut along the ribbon axis in its centre and along its edges showed differences in the onset of structural relaxation according to their different cooling histories during production: the outer parts leaving the melt-spinning wheel earlier than the centre suffer more pre-annealing during air cooling than the latter. Specimens cut perpendicular to the ribbon axis show a definitely smaller amount of structural relaxation than those cut along the ribbon axis, indicating elongated regions of lower density with their long axis oriented along the production direction of the ribbon.

Acknowledgments

Thanks are due to Dr H R Hilzinger, Vacuumschmelze Hanau, for providing the specimen material, and to Professor W Gey and Dr W Eschner for making it possible for us to use their x-ray facilities. The financial support of this work by the Deutsche Forschungsgemeinschaft is gratefully acknowledged.

References

Baro M D, Clavaguera N and Surinach S 1988 *Mater. Sci. Eng.* **97** 333–6
Bothe K 1985a *Proc. RQ5* ed. S Steeb and H Warlimont (Amsterdam: North-Holland) pp 731–4
—— 1985b *Dissertation* Technische Universität Braunschweig
Bothe K, Hansmann M and Neuhäuser H 1985 *Scr. Metall.* **19** 1513–6
Bothe K and Neuhäuser H 1982 *Scr. Metall.* **16** 1053–7
—— 1983 *J. Non-Cryst. Solids* **56** 279–84
Cahn R W, Pratten N A, Scott M G, Sinning H R and Leonardsson L 1984 *Rapidly Solidified Metastable Materials* ed. B H Kear and B C Giessen (New York: North-Holland) pp 241–52
Chen H S 1978 *J. Appl. Phys.* **49** 3289–91
—— 1983 *Amorphous Metallic Alloys* ed. F E Luborsky (London: Butterworth) pp 169–86
Dietz G and Börngen L 1983 *J. Non-Cryst. Solids* **58** 275–84
Dietz G, Hüller K and Jung K 1984 *J. Non-Cryst. Solids* **57** 265–73
Egami T 1983 *J. Magn. Magn. Mater.* **31–34** 1571–74
Fukamichi K 1983 *Amorphous Metallic Alloys* ed. F E Luborsky (London: Butterworth) pp 317–40
Gerling R and Wagner R 1983 *Scr. Metall.* **17** 1129–34
Gibbs M R J, Evetts J E and Leake J A 1983 *J. Mater. Sci.* **18** 278–88
Girt E 1982 *J. Phys. E: Sci. Instrum.* **15** 811–3
Girt E, Kursumovic A and Mihac-Kosanovic T 1980 *J. Phys. E: Sci. Instrum.* **13** 808–900
Girt E, Tomic P, Mihac T and Kursumovic A 1982 *Scr. Metall.* **16** 693–6
Gonser U, Ackermann M and Wagner H-G 1983 *J. Magn. Magn. Mater.* **31–34** 1605–7

Gordelik P 1983 *PhD thesis* University of Stuttgart
Gordelik P and Sommer F 1985 *Proc. RQ5* ed. S Steeb and H Warlimont (Amsterdam: North-Holland) pp 623–6
Grössinger R, Hausberger S, Kirchmayr H, Sassik H, Schotzko Ch, Veider A, Wiesinger G and Wernisch J 1984 *J. Magn. Magn. Mater.* **41** 101–4
Hang Nam Ok and Morrish A H 1981a *J. Phys. F: Met. Phys.* **11** 1495–504
—— 1981b *J. Appl. Phys.* **52** 1835–7
Hilzinger H R 1986 private communication
Hilzinger H R, Hillmann H and Mager A 1979 *Phys. Status Solidi* a **55** 763–9
Huizer E and van den Beukel A 1987 *Acta Metall.* **35** 2843–50
Hygate G and Gibbs M R G 1987 *J. Phys. F: Met. Phys.* **17** 815–26
Janot Chr, George B, Teiblinck D, Marchal G, Tete C and Delcroix P 1983 *Phil. Mag.* A **47** 301–13
Koester U and Herold U 1981 *Glassy Metals I* ed. H-J Güntherodt and H Beck (Berlin: Springer) pp 225–59
Komatsu T, Takeuchi M, Matusita K and Yokata R 1983 *J. Non-Cryst. Solids* **57** 129–36
Kopmann G, Frommeyer G and Nicolai H P 1983 *Z. Metall.* **74** 390–3
Leonardsson L 1983 *Phase Transformations in Crystalline and Amorphous Alloys* ed. B L Mordike (Oberursel: DGM) pp 83–93
—— 1985 *Proc. RQ5* ed. S Steeb and H Warlimont (Amsterdam: North-Holland) pp 1353–6
Morris D G 1983 *Acta Metall.* **31** 1479–1489
—— 1984 *Acta Metall.* **32** 837–49
Müller K and von Heimendahl M 1982 *J. Mater. Sci.* **17** 2525–32
Mulder A L, van der Zwaag S, Huizer E and van den Beukel A 1984 *Scr. Metall.* **18** 515–9
Neuhäuser H, Hansmann M and Bothe K 1985 *J. Phys. E: Sci. Instrum.* **18** 1058–62
Nix F C and McNair D 1941 *Phys. Rev.* **60** 597–605
Nowick A S and Berry B S 1972 *Anelastic Relaxation in Crystalline Solids* (New York: Academic)
Phillips D L 1962 *J. Assoc. Comput. Machin.* **9** 84–97
Pilz O and Ryder R L 1985 *Proc. RQ5* ed. S Steeb and H Warlimont (Amsterdam: North-Holland) pp 377–80
Pratten N A 1981 *J. Mater. Sci.* **16** 1737–47
Primak W 1955 *Phys. Rev.* **100** 1677–89
—— 1960 *J. Appl. Phys.* **31** 1524–33
Reusswig S, Gleichmann R, Zielinski P G, Ast D G and Ray R 1984 *Acta Metall.* **32** 1553–60
Scott M G 1978 *J. Mater. Sci.* **13** 291–6
Sinning H R, Leonardsson L and Cahn R W 1985 *Int. J. Rapid Solid.* **1** 175–97
Sommer F, Haas H and Predel B 1985 *Proc. RQ5* ed. S Steeb and H Warlimont (Amsterdam: North-Holland) pp 627–30
Steeb S and Lamparter P 1985 *J. Physique Coll.* **46** C8 247–53
Steffen B and Liedtke G 1981 *Z. Metall.* **72** 849–53
Steinberg J, Tyagi S and Lord A E Jr 1980a *J. Non-Cryst. Solids* **41** 279–82
—— 1980b *Appl. Phys. Lett.* **37** 618–20
Stubicar M, Babic E, Subasic D, Pavuna D and Marohnic Z 1977 *Phys. Status Solidi* a **44** 339–44
Yavari A R 1985 *Proc. RQ5* ed. S Steeb and H Warlimont (Amsterdam: North-Holland) pp 495–8
Yavari A R and Desre P 1984 *J. Phys. F: Met. Phys.* **14** 291–9
Yavari A R, Hicter P and Desre P 1982 *Proc. RQ4* ed. T Masumoto and K Suzuki (Sendai: Japan Institute of Metals) pp 713–8
Zuercher M-H and Morris D G 1988a *J. Mater. Sci.* **23** 515–22
—— 1988b *Mater. Sci. Eng.* **97** 365–8